Comparison of Resolution and Contrast Performances of Silver Film, Imaging Plate and Scintillator Images in Neutron Radiography

Kevin Alvarado[1*], *Antoine* Drouart[1], and *Frédéric* Ott[2]

[1]IRFU, CEA, Université Paris-Saclay, 91191 Gif-sur-Yvette Cedex, France
[2]LLB, CEA, CNRS, Université Paris-Saclay, 91191 Gif-sur-Yvette, France

Abstract. In the last decades, neutron imaging facilities have implemented systems such as imaging plates and CCD or sCMOS cameras coupled to a scintillator screen [1]. However, for some applications, such as detection of micro cracks in large-size metallic or organic materials such as pyrotechnic equipment, these methods have disadvantages, mostly related to their small field of view when high resolutions are required. On the other hand, the use of silver radiographic films, although an old technology restricted to static 2D imaging, allows observing details with very good spatial resolution (<50 µm) and over very large areas (30x30cm²), which compensates for their low efficiency. Since there is currently no technology that fulfills these needs, radiographic films were used on the Orphée reactor at the CEA Saclay until its shutdown in 2019. The CEA aims at potentially continuing the previous historical radiography activities on a new French HiCANS source, the ICONE project. Within this context, we aim at comparing radiographic films and other technologies. Hence radiographies were taken with films at PSI/SINQ on the NEUTRA beam line (with thermal neutrons, which will probably will be used at the ICONE facility) in order to compare them with measurements on the same objects taken at the Orphée nuclear reactor (with cold neutrons). Images were obtained with different neutron energies, different L/D and different fluence levels. High-resolution digitalization of the film was performed for quantitative analysis. We compared these images to those obtained with imaging plates or CCD cameras. A study of the quality and the statistics of the images after digitalization was done in order to quantify the evolutions of the dynamic range and the spatial resolution. We also aim at evaluating the effect of thermal energies vs cold energies. With these results, it could be determined if the usage of films can complement modern neutron imaging methods to fulfil specific requirements.

1 Introduction

X-ray radiography is a well-known non-destructive method to study the internal structure of materials. X-ray absorption is directly dependant on the atomic number of the elements

* Corresponding author: kevin.alvarado@cea.fr

present in the analysed samples [2] so that the sensitivity to light elements such as hydrogen is low. For this reason, using neutrons instead of X-rays is useful to detect the presence of certain light elements such as hydrogen or boron, especially when these elements are shadowed by a heavy metallic matrix (e.g. iron or lead) or when large metallurgical pieces must be analysed. At the CEA Saclay, the Orphée nuclear reactor was used until 2019 for industrial uses of neutron radiography [2]. The CEA is currently evaluating the possibility of using HiCANS to reproduce the lost capabilities. In particular, the ICONE project [3] is currently proposed as a possible new French neutron scattering facility.

The foreseen flux at ICONE is of the order of about 2×10^6 neutrons/cm²/s, which is, as expected with a CANS, two orders of magnitude lower than the nuclear reactor Orphée's flux (which was about 2×10^8 neutrons/cm²/s). One should also note that the ICONE source would be operated in pulsed mode which not efficient for radiography measurements. Thus, it will be necessary to adapt the neutron radiography techniques to the ICONE low flux while maintaining similar capabilities as on Orphée, mainly a high spatial resolution, of the order of 20-30µm over a field of view (FOV) larger than 400 cm². We are currently investigating and comparing different technological solutions. This communication focusses on silver radiographic films.

2 The set up

In order to compare the G45 cold neutron radiography station at Orphée with a thermal radiography station, reference samples were taken to the SINQ spallation source, at PSI in Switzerland, in May 2022. The samples used to compare the quality of the radiography technologies were pyrotechnic lines with a diameter of about 640 µm in which micro-cracks (with a width down to a few tens of micrometers) need to be identified. The line is embedded in a 1.5 mm lead sheath. The pyrotechnic lines are inside stainless steel tubes with a diameter of about 6 mm. The tubes shown in Figure 1. In these specific samples, cracks were created on purpose with the goal of quantifying the sensitivity of the setup. The cracks extend from the edges of the lines over a few cm along the lines.

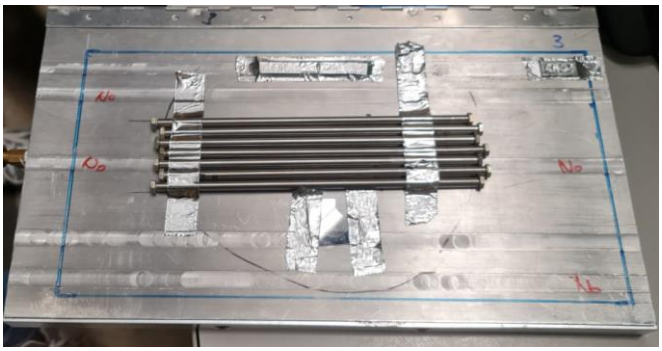

Fig. 1: Set of pyrotechnic lines used as samples for the tests at NEUTRA.

The measurements were made at positions 1 and 2 of the NEUTRA station, which have a different L/D collimation ratio, different field of view and different flux [4,5] (see Table 1). During the experiment, the proton current at PSI was 1.3 mA, so the exact flux ratio is determined from it.

Table 1. Parameters of the two imaging positions at NEUTRA.

Position	L/D	Flux ($cm^{-2}s^{-1}$)	Field of view
1	200	4.8×10^{7}	Circular, 18 cm diameter
2	350	1.3×10^{7}	Rectangular, 24 x 17 cm^2

We aimed at comparing three different radiography techniques:

- Imaging plates (IP) Fujifilm 2040 BAS-ND [6,7], designed for neutron imaging thanks to a gadolinium enriched substrate;
- Silver radiographic films (SRF) AGFA Structurix D3SC [8], laid flat against a glass or aluminium plate, on which a 20µm Gd thin film is used as a neutron convertor;
- CCD camera imaging, using a LiF-ZnS neutron-sensitive scintillating screen, 60×60mm^2 wide and 230 µm thick, read by an ANDOR Ikon-L camera using a Carl Zeiss Makro-Planar 2/100 ZF.2 T* objective, for an effective pixel size of 33µm x 33µm.

The IP images used for this comparison were taken at Orphée in 2019, some new SRF radiographies were taken at NEUTRA to compare them to those taken in 2019 at Orphée, and the CCD radiography was performed at NEUTRA.

Every method has advantages and disadvantages:

- SRF is a very well-known technology. The field of view can be large since the manufactured films are also large and the spatial resolution can be very good (better than 50 µm). However, their sensitivity is quite low, which requires high fluences (on the order a few 2×10^{9} n/cm^2), and they need to be handled carefully since the films degrade in the presence of light. The dynamic range is very limited (1 or 2 orders of magnitude only) which requires a careful control of the measurement conditions to achieve optimal exposure.
- IPs have large active area (20 x 40 cm^2), and they have a much better sensitivity and a very good dynamic range (four to five orders of magnitudes). On the other hand, they also have a large sensitivity to gamma radiation and the effective resolution is limited (of the order of 100 - 150 µm), even for scanning pixel size of 25 µm.
- CCD imagers allows a real-time data acquisition, required for 3D-tomography of time-dependant phenomenon. High spatial resolution is however traded for sensitivity (thinner scintillator) and field of view (at large magnification) [9]. Typically spatial resolution below 50µm requires a nominal pixel size ≈ 20µm which corresponds to a FOV of the order of 40mm for a typical 4 MPixels sCMOS camera. Modern 4K cameras would increase the FOV to 80mm.

The fluences used in the different experiments are listed in the Table 2.

Table 2. Fluences used in the different measurements.

Station	Ranges of Fluence (10^9n.cm^{-2})
Orphée SRF	1.5 (real flux), 7.7 (thermal neutrons equivalent)
Orphée IP	2.6
NEUTRA – Position 1	From 1.5 to 4.5
NEUTRA – Position 2	From 1.6 to 2.3
NEUTRA – CCD	From 0.4 to 0.8

In the case of the fluence at Orphée, the real flux and the equivalent flux by thermal neutrons is indicated. Different radiographies with different fluences were taken at NEUTRA position 1, 2 and with the CCD camera. While the CCD radiographies were taken with a lower fluence, they were taken within the recommendations of PSI operators, and its biggest fluence is still comparable to the lowest SRF fluences.

3 Qualitative differences

We show in Figure 2 the images of the pyrotechnic lines used as samples, the SRF and the CCD radiograhies taken at NEUTRA position 1, and the IP radiography taken at Orphée. In the zoomed parts, we can see the cracks. The contrast and the signal-to-noise ratio is however very different from one measurement to the other, but for the visualization they have artificially been set to similar levels. We can see that the SFR are very noisy, but the fissures are easily distinguishable, the IP is much less noisy but the fissures are harder to distinguish, and the CCD image is also noisy and the contrast is very low.

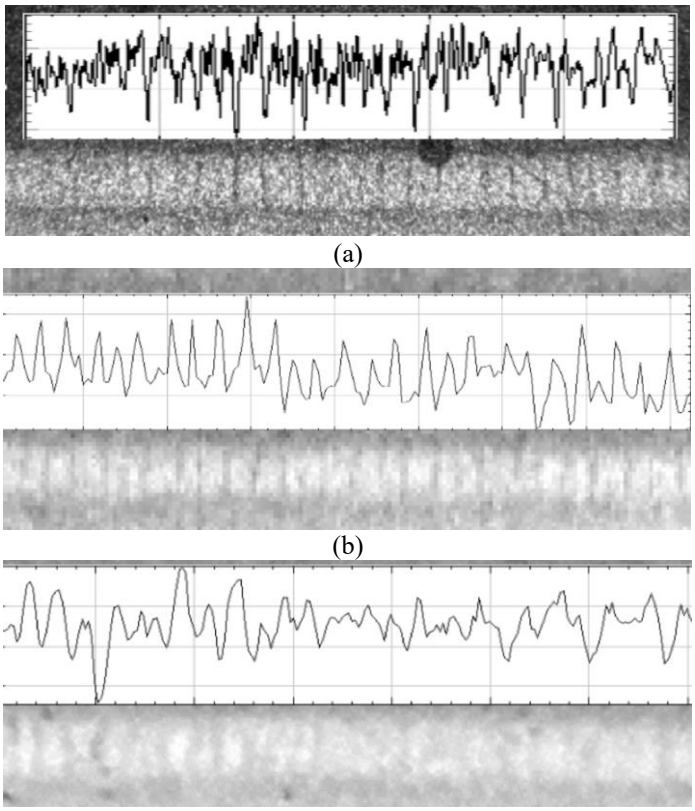

Fig. 2: Comparison of the radiographies of one of the samples, (a) using a SRF at NEUTRA, (b) using an IP at Orphée and, (c) using a CCD camera at NEUTRA. The curves are 2D cuts along the transmission lines. The transmission length that can be seen is 640 µm wide.

4 Resolution and MTF comparison

The spatial resolution can be defined by the modulation transfer functions (MTF), which quantifies the contrast as a function of the features sizes, usually defined in [line pairs/mm] (lp/mm). Spatial resolution was measured using gadolinium Siemens stars. The pattern is the same for all of the Siemens stars. The line pairs per millimetre in the external zone of the pattern is 2 lp/mm, and then increases to 2.5, 3.3, 5, 10 lp/mm at each inner ring (see figure 3).

From the SRF taken at NEUTRA and G45@Orphée, the values of the resolution are around 50 µm, as explained later. On the other hand, the image obtained with the CCD camera is much blurrier, and there is also a noticeable anisotropic artefact due probably to optical aberration of the objective lens.

The figure 4 shows that the Orphée SFR's MTF degrades faster than those on the NEUTRA SRF. A possible explanation is the technology used for the Gd-neutron convertor layer: at Orphée, the Gd is deposited on an aluminium plate, while at PSI it is deposited on a glass plate: the glass plate is expected to be much flatter and smoother that the aluminium one, and so allows a better contact between the Gd layer and the SRF. The SRF is imprinted by the secondary electrons coming from the Gd after neutron capture. For that reason the distance between the Gd and the film is critical, and has a direct effect on the spatial resolution. The flatness defects of the aluminium plate would thus deteriorate the spatial resolution. In the cases of the CCD image and the IP image, the MTF drops quickly.

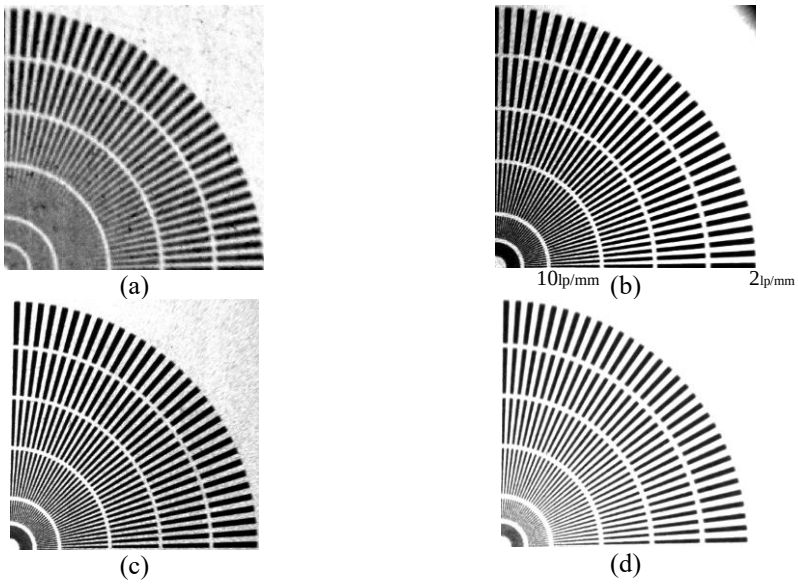

Fig. 3: Comparison of the Siemens stars obtained by (a) the CCD camera (b) a SRF at NEUTRA position 1 (c) a SRF at NEUTRA position 2 and (d) a SRF at Orphée for SRFs with similar optical density. The radius of all the stars are equal to 10 mm, and the contrast were amplified for better comparison.

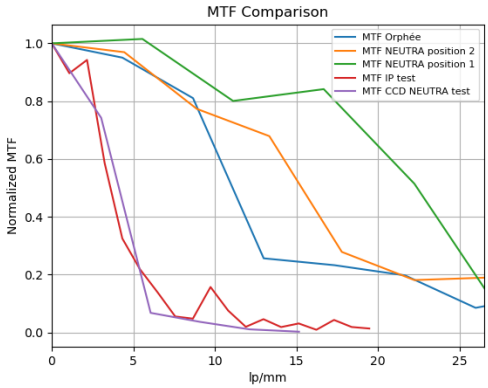

Fig. 4: MTF curves for the SRF and CCD image at NEUTRA and SRF and IP at Orphée calculated from the Siemens star measurements.

We define the "resolution" as the spatial period (i.e. inverse of lp/mm) where the MTF reaches a value of 0.2. The resolution values obtained from the figure 4 are shown in the table 3.

For the CCD camera, the image obtained has a limited resolution of about 150 µm, which is expected considering the 230µm thick scintillator screen. One could consider to lower the screen thickness, but this would reduce the detection efficiency for the former.

For the IP image, the spatial resolution is of the order of 140µm, due to the 150µm thickness of the active layer of the IP BAS-ND. Unfortunately, no other IP models with reduced thickness are commercially available.

For SRF, the resolution is on the order of 50 µm. Note that in this configuration, no difference is observed between the measurement with cold neutrons (Orphée) and thermal neutrons (NEUTRA).

Table 3: Resolution comparison from the different imaging systems

Imaging station	Resolution (µm)
NEUTRA CCD	174
Orphée IP	143
Orphée SRF	47
NEUTRA Position 2	From 30 to 47
NEUTRA Position 1	From 32 to 45

5 Local contrast, dynamic range and signal-to-noise ratio for SRF

The opacity of the SRF generated by radiation is expressed in terms of optical density, this is related to grey levels in a digitalized image through the relation:

$$D = \log\left(I_{\text{transmitted}}/I_{\text{incident}}\right) \quad (1)$$

Where D is the optical density, $I_{\text{transmitted}}$ and I_{incident} are the intensities of the incident and transmitted light on the film. For a static image, the grey level G registered in a pixel of the

digitalized image will be proportional to the total light intensity received by the sensor, and this can be used for comparing optical densities through different parts of the image.

The Weber contrast for a given object surrounded by a homogeneous background is defined as the ratio of the difference of grey levels, between the object and the background, and the background [10]. For this context, the open beam is considered as the image background, and since it has the lower grey level, it allows using a simpler definition of a local contrast:

$$C_{\text{local}} = G_{\text{object}}/G_{\text{open beam}} \quad (2)$$

Where G_{object} and $G_{\text{open beam}}$ are the grey levels of the digital images of the object and the open beam respectively. The local contrast is a tool for background correcting the digitalized SRF radiographies and also to evaluate the neutron opacity from the samples. Agfa Structurix D3SC films have a linear dependency between optical density and neutron fluence for optical densities bellow 4.5 [8].

For this study, the grey levels were compared in the pyrotechnic lines and in a direct beam zone, as seen in figure 5, to see how the neutron fluence affects the contrast.

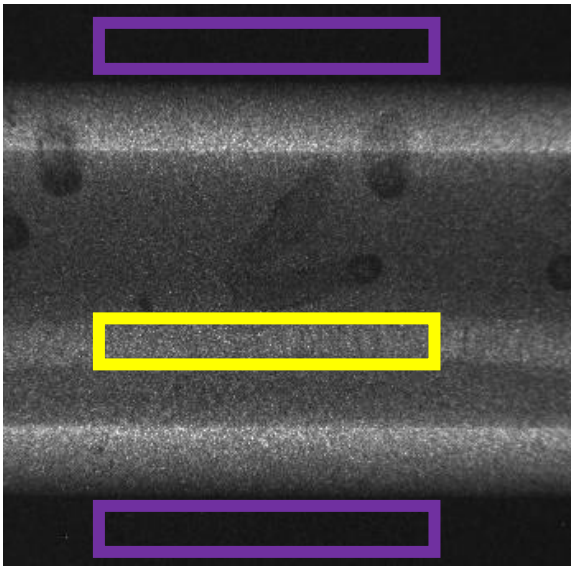

Fig. 5: Portion of image where the pyrotechnic line (yellow rectangle in the middle) and the direct open beam (purple rectangle in the up and down zones) are seen. The contrast of the images is inverted. Dark regions (purple rectangles) correspond to “open beam” or “empty beam” regions. They allow calibrating the absolute transmission (T=1). The steel tube that can be seen between the open beam regions has a width of 6 mm.

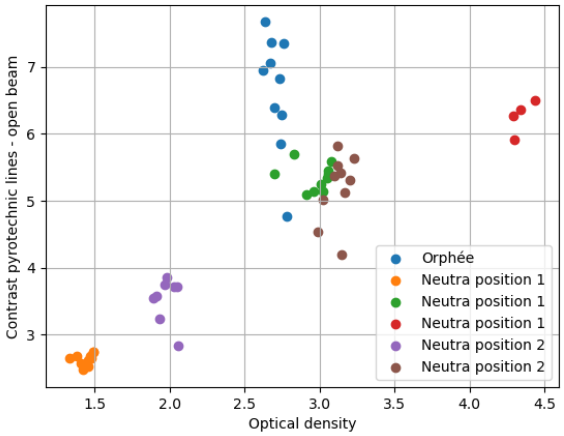

Fig. 6: Relation between the contrast and the optical density of the SRF. The diferent points are measures along the pyrotechnic lines for different films, close to the optical densities of the open beam. Different colors correspond to different films with different fluences

The optical density has been measured using a densitometer in open beam regions next to the regions where the gray level of pyrotechnic lines are measured. Different colors show different radiographies. As seen in Figure 6, the contrast improves with the optical density, which is proportional to the neutron fluence since their values are in the region of linear behavior [8]. This shows that, while a good spatial resolution can also be obtained with lower fluences, the contrast keeps increasing with the total neutron dose, which improves the identification of certain defects in the objects present in the radiography. We also see that for similar optical density values, the contrast obtained at Orphée is better than those obtained at NEUTRA. This is a result of the different neutron energy spectra: cold neutrons are more easily absorbed or scattered at high angles than more energetic neutrons, leading to lower grey levels behind the object and consequently a better contrast.

SRF are known to have a limited dynamic range, less than a decade for Agfa Structurix D3SC films [8]. In our measurements, we operated with fluences within a factor 3 (from D=1.5 to 4.5) in the upper range of the film specifications. Within that range, the optical density is linear with the neutron fluence. Moreover, we did not observe the film saturation that is expected around D=3.5, and our contrast keeps improving up to D=4.5.

A different parameter to evaluate the quality of the region of an image is the signal to noise ratio (SNR), which is derived from the grey levels distribution in a homogeneous grey level region of the image. It is defined by:

$$SNR = 10 \log G_{\text{signal}}/\sigma(G_{\text{signal}}) \quad (3)$$

Where G_{signal} and $\sigma(G)_{signal}$ are the grey level of the signal and its standard deviation respectively, and the SNR is measured in dB. This quantity expresses how noisy an image is: the larger the SNR, the lower the noise. The signal and noise are estimated from a local uniform region such as the zone directly hit by the beam, or the interior of a tube, the signal is the mean of the grey levels and the noise is the standard deviation. The table 2 shows the

comparison between the different values of SNR for films with similar open beam optical densities.

Table 4: Signal to noise ratios for the different SRF measurements

Measurement station	SNR
Orphée (2019)	7.1 dB
PSI – NEUTRA position 1	6.4 dB
PSI – NEUTRA position 2	6.4 dB

From these results, it can be inferred that cold neutrons give similar or better SNR than thermal neutrons, which is consistent with the energy spectra of both kind of beams.

6 Conclusions and perspectives

Considering the specific studied samples, SRF are still a competitive solution when it comes to having high (≈50µm) spatial resolution over large surfaces, when only 2D, static images are required. Despite their high efficiency, the imaging plates are limited by their intrinsic poor (≈140µm) spatial resolution. A proper CCD+scintillator screen configuration could reach the 50µm resolution, and even better, but then its sensitivity decreases (due to the very low thickness of the screen) and the field of view becomes very small (due to the magnification on the CCD). Such a setup is no more competitive with radiographic films in terms of global efficiency. While these conclusions apply for our specific needs (pyrotechnic components), SRF are definitively not suited for applications such as tomography or time resolved measurements. For this reason, it is still necessary to implement modern imaging technologies, as well as modern imaging treatment techniques.

References

1. E. Lehman, P. Trtik, D. Ridikas, Physics Procedia **88**, 140 – 147 (2017)
2. Neutron radiography : non destructive testing. Available at: https://www-llb.cea.fr/neutrono/nr1.html. (Accessed: 15th January 2024)
3. 1.Icone : An accelerator-driven neutron source (2023). Available at: https://iramis.cea.fr/llb/Phocea/Vie_des_labos/Ast/ast_sstechnique.php?id_ast=2755. (Accessed: 15th January 2024)
4. NEUTRA: NEUtron Transmission Radiography. Available at: https://www.psi.ch/en/sinq/neutra. (Accessed: 15th January 2024)
5. E. H. Lehman, P. Vontobel, L. Wiezel, Nondestr. Test. Eval., **16**, 191-202 (2001)
6. K. Takahashi, S. Tazaki, J. Miyihara, Y. Karasawa, N. Niimura, Nuc. Instr. and Meth. in Phys. Res. A **377**, 119-122 (1996)
7. E. Simon, P. Guimbal, EPJ Web Conf. **170**, 04021 (2018)
8. N. E. Lanier, J. S. Cowan, Rev. Sci. Instrum. **85**, 11D632 (2014)
9. E. H. Lehman, A. Tremsin, C. Grünzweig, I. Johnson, P. Boillat, L. Josic, JINST **6** C01150
10. E. Peli, J. Opt. Soc. Am. A **7**, 2032-2040 (1990)